Thermochimica Acta 512 (2011) 202–207

Contents lists available at ScienceDirect

Thermochimica Acta

journal homepage: www.elsevier.com/locate/tca

Thermogravimetric analysis-mass spectrometry (TG-MS) of selected Chinese palygorskites—Implications for structural water

Hongfei Cheng[a,b,c], Jing Yang[b], Ray L. Frost[b,*]

[a] School of Mining Engineering, Inner Mongolia University of Science & Technology, Baotou 014010, China
[b] Chemistry Discipline, Faculty of Science and Technology, Queensland University of Technology, 2 George Street, GPO Box 2434, Brisbane, Queensland 4001, Australia
[c] School of Geoscience and Surveying Engineering, China University of Mining & Technology, Beijing 100083, China

ARTICLE INFO

Article history:
Received 24 June 2010
Received in revised form 3 October 2010
Accepted 14 October 2010
Available online 27 October 2010

Keywords:
Thermogravimetry
Palygorskite
Decomposition
Mass spectrometry

ABSTRACT

Four Chinese palygorskites clay minerals have been analysed by thermogravimetric analysis-mass spectrometry and X-ray diffraction. The structural water of the palygorskite dehydrates in the temperature range of 30–625 °C, as shown in the thermogravimetric analysis and mass spectrometric curves. The mass spectrometric curves combined the differential thermogravimetric curves enable the detailed determination of the main dehydration steps. The results show that the dehydration occurs in four main steps: (a) elimination of interparticle water and partial zeolitic water at below 110 °C, (b) release of the rest part of zeolitic water from the structural layer of palygorskite at about 160 °C, (c) dehydration of one part of bound water at about 340 °C and (d) loss of the rest part of bound water at around 450 °C. The temperatures of dehydration of the palygorskite minerals are found to be influenced by the geological environment and the amount and kind of impurities. The evolved gases in the decomposition process are various because of the different amounts and kind of impurities. It is also found that decarbonization takes place at around 600 °C due to the decomposition of calcite and dolomite impurities in these minerals. It is evident by the mass spectrometric curve that the water is given out from the samples and carbon dioxide originates from the impurity calcite and dolomite.

1. Introduction

Interest in the chemistry of palygorskite stems from a number of reasons. Firstly, palygorskite is one of the very important and valuable industrial clay minerals with a wide range of applications. These applications include their use as catalysts or catalyst supports filler in polymer composites membranes for ultrafiltration specific adsorbent of organic molecules [1–7]. These applications imply the value of the palygorskite at present or in future. Secondly, the structure of palygorskite is very special. Technological applications are based on its physicochemical properties, among others, and especially in its structure. Therefore, it is of high importance to understand well the structure of palygorskite. Thirdly, palygorskite is important from an environmental point of view. Palygorskites are minerals which can function as collectors of heavy metals and other pollutant [8]. Interest in such minerals and their thermal stability rests with the possible identification of these minerals and related dehydrated phyllosilicate related mineral [9]. Many studies on differential thermal analysis and application studies of some related minerals have been published [10–14]. Study on their chemistry composition and thermal analysis has proven extremely useful for determining the stability of minerals [15–20].

Palygorskite is widely applied in many fields of material industry, particularly as oil refining, wastewater treatment, removal of odor, drug, pesticide carriers, catalysts, paper and detergent industries [1–4]. Moreover, palygorskite has received relatively much attention as a polymer reinforcement agent with many studies being devoted to composites of polyolefins, polyurethane, polyimide and polyamide [21]. Therefore, the variety of industrial applications has motivated a vigorous research effort which has revealed concurrent dramatic enhancements for many materials. Palygorskite samples with different physicochemical properties can be obtained through heat treatment and acid treatment [22]. For example, heat treatment can affect the specific surface area of palygorskite, and then has some influence on adsorption capacity of palygorskite. Based on the above considerations, it is necessary to investigate the effect of heat treatment on the all aspect properties of palygorskite in mineral system. In general, the industrial raw palygorskite from China is a mixture of minerals, which contains different non-clay minerals besides major and minor clay minerals. The palygorskites clays from China with the major clay mineral palygorskite include minor carbonates with dolomite and calcite as non-clay minerals [23]. Therefore, it is highly interest to study the thermal behavior of palygorskites from China.

---

* Corresponding author. Tel.: +61 7 3138 2407; fax: +61 7 3138 1804.
E-mail address: r.frost@qut.edu.au (R.L. Frost).

0040-6031/$ – see front matter © 2010 Elsevier B.V. All rights reserved.
doi:10.1016/j.tca.2010.10.008

Thermal analysis using thermogravimetric analysis-mass spectrometry enables the mass loss steps, the temperature of mass loss and the mechanism for the mass loss to be determined. Although the thermal behavior of the palygorskite have been studied by thermogravimetric techniques [23,24], thermogravimetric-mass spectrometry methods can provide evidence for the products of thermal decomposition [25]. This paper, based on author's previous work [19], reports the steps of dehydration of four palygorskites from China using X-ray diffraction (XRD) and thermogravimetric-mass spectrometry (TG-MS). The purpose of the present study is to make clear the dehydration process of palygorskite with respect to the removal of structural water.

2. Experimental methods

2.1. Materials

Four palygorskite samples, containing impurities quartz, dolomite and calcite, were selected for this study (Table 1). It was reported that particle size distribution produces a significant influence in the thermal behavior of clays such as significant shifts in the dehydration temperature or in the percentage of hydration structural water [26–28]. Therefore, the samples were used directly, without prior size fraction separation, since one of the objectives was to determine the influence on the thermal behavior of mineral samples.

2.2. X-ray diffraction

X-ray diffraction patterns were collected using a PANalytical X'Pert PRO X-ray diffractometer (radius: 240.0 mm). Incident X-ray radiation was produced from a line focused PW3373/10 Cu X-ray tube, operating at 40 kV and 40 mA, with Cu Kα radiation of 1.540596 Å. The incident beam passed through a 0.04 rad soller slit, a 1/2° divergence slit, a 15 mm fixed mask, and a 1° fixed antiscatter slit.

2.3. Thermogravimetric analysis and mass spectrometry

Thermogravimetric analysis (TG) of the samples was carried out in a TA® Instruments incorporated high-resolution thermo gravimetric analyzer (series Q500) in a flowing nitrogen atmosphere ($60\,cm^3\,min^{-1}$). Approximately 50 mg of each sample underwent thermal analysis, with a heating rate of 5 °C/min, with resolution of 6, from 25 °C to 750 °C. The TG instrument was coupled to a Balzers (Pfeiffer) mass spectrometer for gas analysis. Only water vapour, carbon dioxide, carbon and oxygen were analysed. In the MS figures, e.g. Fig. 3, a background of broad peaks may be observed. This background occurs for all the ion current curves. The background becomes more prominent as the scale expansion is increased. It is considered that this background may be due to the loss of chemicals which have deposited in the capillary which connects the TA instrument to the MS.

3. Results and discussion

3.1. X-ray diffraction (XRD) and structure of palygorskite

The XRD patterns of the four selected palygorskite minerals with standard XRD patterns are shown in Fig. 1. They show that the mineral compositions within these four palygorskite samples are various, and the notable difference between these samples is the occurrence of some impurity. F-1 and G-1 samples show almost pure palygorskite. Sample H-1 contains significant amounts of calcite impurity, however, while Z-1 contains dolomite. The XRD patterns of representative clay separates of these four samples reveal that these four samples have similar clay mineral compositions, consisting mainly of palygorskite. Changes in the relative proportions of the clay minerals are seen from Fig. 1.

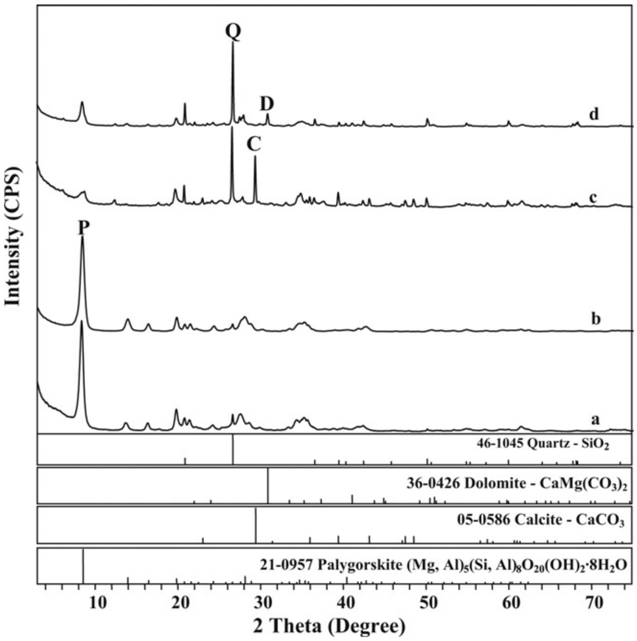

Fig. 1. XRD patterns for palygorskite samples (a) F-1, (b) G-1, (c) H-1, (d) Z-1 and reference patterns: JCPDS card No. 21-0957 Palygorskite (P), No. 05-0586 Calcite (C), No. 36-0426 Dolomite (D) and No. 46-1045 Quartz (Q).

Palygorskite, with the chemical composition $(Mg, Al)_5(Si, Al)_8O_{20}(OH)_2(OH_2)_4\cdot 4H_2O$, is a crystalline hydrated magnesium silicate with a fibrous morphology. Palygorskite and, less commonly, sepiolite are fibrous clay minerals reported in soils of arid and semiarid regions [15,29,30]. The structure of palygorskite contains ribbons of 2:1 phyllosilicates linked by periodic inversion of the apical oxygen of the continuous tetrahedral sheet every four atoms of Si (two tetrahedral chains). The tetrahedral sheet is continuous across ribbons but the octahedral sheet is discontinuous as a result of the periodic inversion, and terminal octahedral cations must complete their coordination sphere with water molecules [31]. As reported by Frost [19] and Suarez [32], in the structure of palygorskite, four water molecules are bonded by two per two the first and Mg^{2+} cations at the both ends of each ribbon and located in nanopores.

3.2. Thermogravimetric analysis

To investigate the dehydration process of palygorskite, the thermogravimetry and differential thermogravimetric (TG–DTG) analyses of the palygorskite minerals are presented in Fig. 2a–d, which show the TG–DTG curves for these four samples. The dehydration process for these four palygorskite minerals are discussed in details as followed.

Fig. 2a shows the dehydration process for F-1. There are four main mass losses in TG curve of this sample. The first mass loss of 8.85% is observed at below 110 °C. This mass loss is attributed to be the elimination of interparticle water and one part of zeolitic water. The similar results were reported by Yener [23]. However, they found that the first and major mass loss of palygorskite occurred between 25 and 190 °C with the maximum rate at 83 °C, and this temperature range of losing these types of water is different from our finding. This may be due to the various resolutions of thermogravimetric analyzers. The second mass loss is observed at 148 °C with a mass loss of 3.44%, which is assigned to the thermal dehydration of the rest part of zeolitic water from the structural layer of the palygorskite. The third mass loss is observed at 347 °C with

Table 1
Palygorskite samples from China.

Palygorskite samples	Location	Content of clay mineral	Impurities
Palygorskite (F-1)	Feidong, Anhui Province of China	Palygorskite	Quartz
Palygorskite (G-1)	Guanshan, Anhui Province of China	Palygorskite	Quartz,
Palygorskite (H-1)	Hefei, Anhui Province of China	Palygorskite	Quartz, calcite
Palygorskite (Z-1)	Zhangze, Jiangsu Province of China	Palygorskite	Quartz, dolomite

mass losses of 2.3%, which is due to loss of one part of bound water. The last mass loss is observed at 414 °C with mass losses of 4.02%, which is attributed to loss of the rest part of bound water. It was reported by Nagata et al. [17] that the bound water of palygorskite is removed in two steps. Four major mass losses are observed on the TG curve for the sample G-1 (Fig. 2b). These steps are similar to the dehydration of structural water for F-1. The four dehydration steps, which correspond to mass losses of 9.12% (room temperature to 110 °C), 3.2% (125–175 °C), 2.2% (300–375 °C) and 3.28% (375–500 °C), are assigned to the elimination of interparticle water and partial zeolitic water, release of the rest part of zeolitic water from the structural layer of the palygorskite, dehydration of one part of bound water and loss of the rest part of bound water. These results are in good agreement with the literature recording the dehydration of palygorskite [19,33–36]. Four major mass losses are clearly observed at maxima of 51, 172, 341 and 422 °C. However, the thermal behavior of other natural palygorskite samples of different origins and with different amounts of impurities is different.

In Fig. 2c, three distinct mass losses are observed in the TG–DTG curves of H-1 mineral sample. The TG–DTG curve of this palygorskite, with impurity calcite, presented a peak at 155 °C associated with dehydration of the zeolitic water with a mass loss of 0.52%. The second peak appeared at 431 °C, accompanied by a mass loss of 0.24% caused by loss of bound water. Another mass loss is observed at 603 °C with a mass loss of 37.41%. This step can be interpreted as being due to the thermal decomposition of impurity calcite. Unlike the thermal behavior of sample H-1, there are five different mass losses in sample Z-1 (Fig. 2d), the first mass losses of 3.91% between 30 and 110 °C with a maximum at 50 °C is due to the elimination of interparticle water and partial zeolitic water. The second mass loss of 1.26% between 125 and 180 °C with a maximum rate at 160 °C is attributed to the dehydration of the rest part of zeolitic water. The third mass loss of 2.13% between 325 and 450 °C with a maximum rate at 421 °C is assigned to the dehydration of the first part of bound water. According to the evolution of gas species from MS spectra in Fig. 3d, the fourth mass loss of 2.09% between 450 and 570 °C is originated from the loss of the rest part of bound water for palygorskite and partial decomposition of impurity dolomite. The last mass loss of 2.18% at 576 °C is observed, which is attributed to the thermal decomposition of impurity dolomite.

Changes in the mineral composition of these four palygorskites result in the different thermal decomposition properties. In general, the dehydration of palygorskite takes place in four steps including elimination of interparticle water and partial zeolitic water at below 110 °C, release of the rest part of zeolitic water at about 160 °C, dehydration of the first part of bound water at about 340 °C and loss of the rest part of bound water at about 450 °C. Therefore, the zeolitic water and bound water for palygorskite is removed in two steps, respectively. Comparing these four palygorskite minerals, both F-1 and G-1, with minor impurity quartz, show the typical dehydration as above. However, palygorskites, regardless of the content of mainly composition, exhibited a remarkable change in the temperature of dehydration of bound water for the palygorskite minerals H-1. This may be due to the existence of impurity calcite. In sample Z-1, the palygorskite, with impurity of dolomite, have a different thermal behavior with the other palygorskite samples. These results suggest that the thermal dehydration of palygorskite minerals is decided not only by the main physicochemical properties of palygorskite, but also by the mount and kind of impurities.

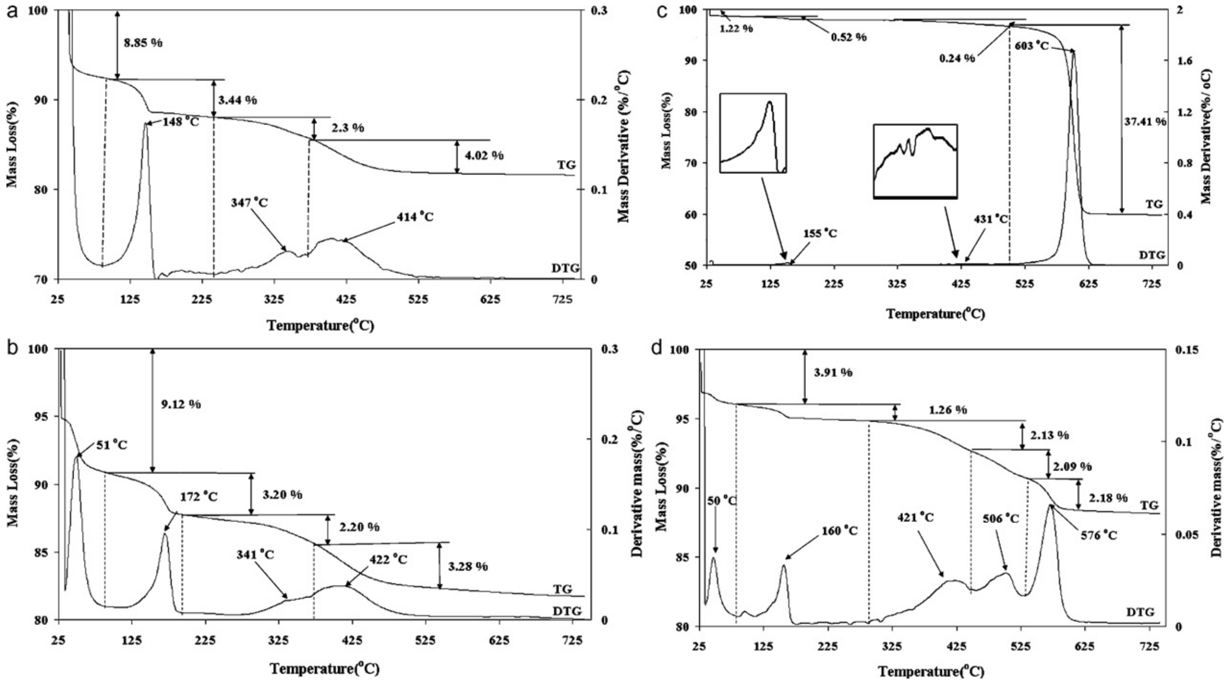

Fig. 2. TG–DTG curves for palygorskite samples (a) F-1, (b) G-1, (c) H-1, (d) Z-1.

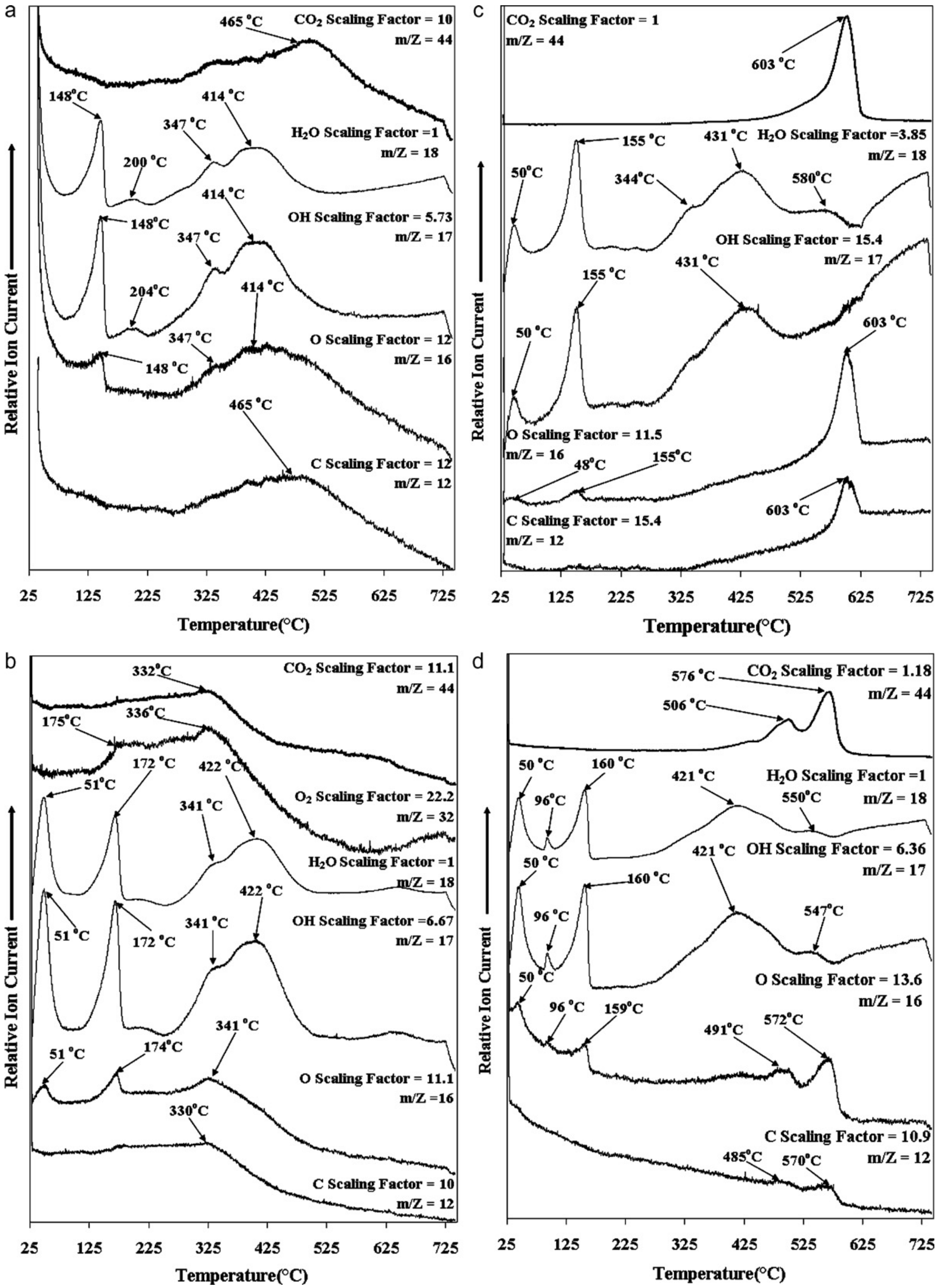

Fig. 3. Evolved gas analysis for palygorskite samples (a) F-1, (b) G-1, (c) H-1, (d) Z-1.

3.3. *Mass spectrometric analysis*

In accordance with former findings several different steps of dehydration have occurred. In order to clarify the thermal decomposition mechanism of palygorskite and understand well the dehydration of structural water for Chinese palygorskite minerals, the mass loss during each decomposition process should be characterized by the identified evolution components. The mass spectrometric data also provide evidence on the thermal decomposition products and mainly chemical composition.

The interpretation of the mass spectra occurs on the basis of degassing profiles from the molecule ions of water (H_2O^+: $m/Z = 18$), carbon dioxide ($CO_2{}^+$: $m/Z = 44$) as well as by fragment ions (OH^+: $m/Z = 17$, O^+: $m/Z = 16$ and C^+: $m/Z = 12$).

The evolution of gas species has been followed in situ by the coupled TG-MS system. The evolution curves of ion-fragments of various gases released are shown as ion current versus temperature curves in Fig. 3a–d. For convenience, these four minerals are divided into two groups to analysis. According the XRD results, they are divided into (a) palygorskite with minor impurity quartz and (b) palygorskite with other impurities. The XRD patterns of these four minerals reveal that samples F-1 and G-1 have similar clay mineral composition, consisting mainly of palygorskite and minor quartz. Four major thermal decomposition steps are observed. The first step at below 110 °C is due to loss of the interparticle water and one part of zeolitic water for these two palygorskite samples. This reaction can be represented as below:

$$(\mathrm{Mg, Al})_5(\mathrm{Si, Al})_8\mathrm{O}_{20}(\mathrm{OH})_2(\mathrm{OH}_2)_4 \cdot 4\mathrm{H}_2\mathrm{O}$$
$$\rightarrow (\mathrm{Mg, Al})_5(\mathrm{Si, Al})_8\mathrm{O}_{20}(\mathrm{OH})_2(\mathrm{OH}_2)_4 + 4\mathrm{H}_2\mathrm{O}$$

The characterization of water release by means of mass spectra is possible with the molecule ion H_2O^+ ($m/Z = 18$) together with the fragment ion OH^+ ($m/Z = 17$) and O^+ ($m/Z = 16$). Because the interparticle water and one part of zeolitic water are removed in same temperature range, the overlapping mass loss for this step should be more than the theoretical value (8.52%) of dehydration for palygorskite. Peaks at 148 °C for F-1 and at 172 °C for G-1 are found in the ion current curve for H_2O^+ ($m/Z = 18$); corresponding peaks are also found in the ion current curves for OH^+ ($m/Z = 17$) and O^+ ($m/Z = 16$). It can be safely concluded that the water is given out at about 148 °C for F-1 and at 172 °C for G-1 from the samples. This reaction can be represented as below:

$$(\mathrm{Mg, Al})_5(\mathrm{Si, Al})_8\mathrm{O}_{20}(\mathrm{OH})_2(\mathrm{OH}_2)_4$$
$$\rightarrow (\mathrm{Mg, Al})_5(\mathrm{Si, Al})_8\mathrm{O}_{20}(\mathrm{OH})_2(\mathrm{OH}_2)_{2.5} + 1.5\mathrm{H}_2\mathrm{O}$$

The theoretical mass loss for this step is 3.19% compared with the observed value of 3.44% for F-1 and 3.2% for G-1, these results are in excellent agreement with the theoretical value.

The third step at 347 °C for F-1 and at 341 °C for G-1 is assigned to the dehydration of the first part of bound water. The dehydration also can be proved by the ion current curves for OH^+ ($m/Z = 17$) and O^+ ($m/Z = 16$). Therefore, this phase can be represented as below:

$$(\mathrm{Mg, Al})_5(\mathrm{Si, Al})_8\mathrm{O}_{20}(\mathrm{OH})_2(\mathrm{OH}_2)_{2.5}$$
$$\rightarrow (\mathrm{Mg, Al})_5(\mathrm{Si, Al})_8\mathrm{O}_{20}(\mathrm{OH})_2(\mathrm{OH}_2)_{1.5} + \mathrm{H}_2\mathrm{O}$$

This step theoretical mass loss should be 2.12% and the values of 2.3% for F-1 and 2.2% for G-1 are observed.

The last step at 414 °C for F-1 and at 422 °C for G-1 is assigned to the loss of the rest part of bound water for the palygorskite. This reaction can be represented as below:

$$(\mathrm{Mg, Al})_5(\mathrm{Si, Al})_8\mathrm{O}_{20}(\mathrm{OH})_2(\mathrm{OH}_2)_{1.5}$$
$$\rightarrow (\mathrm{Mg, Al})_5(\mathrm{Si, Al})_8\mathrm{O}_{20}(\mathrm{OH})_2 + 1.5\mathrm{H}_2\mathrm{O}$$

The last mass loss step should be 3.19%; 3.28% for G-1 is found. The small peak at 498 °C for F-1 is found in the ion current curve for $CO_2{}^+$ ($m/Z = 44$); corresponding peak is also found in the ion current curves for C^+ ($m/Z = 12$). This illustrate a tiny proportion of CO_2 is given out in this temperature range. Therefore, the mass loss observed in this step for F-1 is 4.02%. Thus, there is reasonable agreement with the predicted and the observed mass loss value in this step.

These phase transformations are expressed in the form of chemical reaction for the ease of explanation. The XRD patterns of these four palygorskite samples reveal that the sample H-1 contains mainly of palygorskite and some other impurities, such as quartz and calcite. One addition thermal decomposition step is observed in this sample, excepting the thermal decomposition of the palygorskite. The steps at 50, 155, 344 and 431 °C for H-1 are observed, which is the same as the dehydration of palygorskite. The ion current curves for the evolved gases show for $m/Z = 44$ a mass gain at around 603 °C, attributed to decompose of impurity calcite (Fig. 3c). This reaction can be represented as below:

$$\mathrm{CaCO}_3 \rightarrow \mathrm{CaO} + \mathrm{CO}_2$$

Similar to the XRD pattern analysis of sample H-1, the samples Z-1 consists mainly of palygorskite and some other impurities, such as quartz and dolomite. Besides the thermal decomposition steps of the palygorskite mentioned above, the steps at 576 °C for Z-1 is due to the thermal decomposition of dolomite. This reaction can be represented as below:

$$\mathrm{MgCO}_3 \cdot \mathrm{CaCO}_3 \rightarrow \mathrm{MgO} + \mathrm{CaO} + 2\mathrm{CO}_2$$

It is generally considered that the $CaCO_3$ decomposes nominally at 898 °C, but in silicate minerals generally at 600–700 °C [37,38]. However, the difference in the temperatures of released CO_2 is due to the different percentages of $CaCO_3$ and $MgCO_3$ impurity in these two minerals.

The comparison of these four minerals is shown that the thermal decomposition of these samples is determined by different factors, such as mineral impurities and different locations. The mass gain in the MS curves corresponds precisely with the mass loss in the TG curves.

The present results allow making the conclusion that combination TG and MS is a powerful technique to follow the decomposition process and detect the thermal decomposition products. At the same time, it can be easily detect the impurity in the samples which contain the carbonate. Therefore, this founding is quite important for studying minerals, especially clay minerals, because the nature clay from China always contain carbonate component.

4. Conclusions

The thermal decomposition of four palygorskite minerals collected from different areas of China has been examined using TG-MS, which is proves to be a very useful technique for determining the decomposition products and stability of these minerals. The palygorskite minerals show in general four thermal decomposition steps attributed to dehydration. These steps correspond to (a) the loss of interparticle water and partial zeolitic water (b) release of the rest part of zeolitic water (c) dehydration of the first part of bound water and (d) loss of the rest part of bound water. The thermal behavior of natural palygorskite samples of different origins and with different amounts of impurities is different from the pure palygorskite. The TG-MS have detected and monitored definitely thermally evolved H_2O ($m/Z = 18$) and CO_2 ($m/Z = 44$) from the samples. Anyhow, the $m/Z = 18$ is also the most intense fragment of H_2O, while $m/Z = 44$ fragments arise from impurities. The temperature of dehydration of palygorskite is influenced by the geological environment and the amount and kind of impurities. Therefore, the reproducibility of measurement and richness of qualitative information should be simultaneously considered for proper selection of analysis method for mineral analysis.

Acknowledgment

The authors gratefully acknowledge the financial support provided by the National Natural Science Foundation of China (51034006) and infra-structure support of the Queensland University of Technology Chemistry Discipline, Faculty of Science and Technology. The authors also thank anonymous reviewers for their valuable comments that improved the manuscript.

References

[1] M.E. Sedaghat, M. Ghiaci, H. Aghaei, S. Soleimanian-Zad, Appl. Clay Sci. 46 (2009) 131–135.
[2] M. Onal, Y. Sarikaya, Appl. Clay Sci. 44 (2009) 161–165.
[3] S. Kocaoba, Desalination 244 (2009) 24–30.
[4] Z.-Q. Lei, S.-X. Wen, Eur. Polym. J. 44 (2008) 2845–2849.
[5] J.L. Valentín, M.A. López-Manchado, A. Rodríguez, P. Posadas, L. Ibarra, Appl. Clay Sci. 36 (2007) 245–255.
[6] M. Alkan, M. Dogan, Y. Turhan, Ö. Demirbas, P. Turan, Chem. Eng. J. 139 (2008) 213–223.
[7] E. Franchini, J. Galy, J.-F. Gérard, J. Colloid Interface Sci. 329 (2009) 38–47.
[8] E. Alvarez-Ayuso, A. Garcıa-Sanchez, J. Hazard. Mater. 147 (2007) 594–600.
[9] R.L. Frost, D. Wain, J. Therm. Anal. Calorim. 91 (2008) 267–274.
[10] D. Galusek, Z. Lences, P. Sajgalik, R. Riedel, J. Min. Metall. Sect. B: Metall. 44 (2008) 35–38.
[11] G. Meng, Z. Xu, X. Qi, W. Yang, Z. Xie, Gongye Cuihua 15 (2007) 1–5.
[12] A. Leszczynska, K. Pielichowski, J. Therm. Anal. Calorim. 93 (2008) 677–687.
[13] A.J. Locke, W.N. Martens, R.L. Frost, Thermochim. Acta 459 (2007) 64–72.
[14] L.K. Joseph, H. Suja, G. Sanjay, S. Sugunan, V.P.N. Nampoori, P. Radhakrishnan, Appl. Clay Sci. 42 (2009) 483–487.
[15] G.E. VanScoyoc, C.J. Serna, J.L. Ahlrichs, Am. Miner. 64 (1979) 215–223.
[16] C. Serna, G.E. VanScoyoc, J.L. Ahlrichs, Am. Miner. 62 (1977) 784–792.
[17] R. Nagata, S. Shimoda, T. Sudo, Clays Clay Miner. 22 (1974) 285–293.
[18] W. Kuang, C. Detellier, Can. J. Chem. 82 (2004) 1527–1535.
[19] R.L. Frost, Z. Ding, Thermochim. Acta 397 (2003) 119–128.
[20] J.E. Post, D.L. Bish, P.J. Heaney, Am. Miner. 92 (2007) 91–97.
[21] Y. Chen, Y. Zhao, S. Zhou, X. Chu, L. Yang, W. Xing, Appl. Clay Sci. 46 (2009) 148–152.
[22] D.M. Araujo Melo, J.A.C. Ruiz, M.A.F. Melo, E.V. Sobrinho, A.E. Martinelli, J. Alloys Compd. 344 (2002) 352–355.
[23] N. Yener, M. Önal, G. Üstünışık, Y. Sarıkaya, J. Therm. Anal. Calorim. 88 (2007) 813–817.
[24] H. Bayram, M. Oenal, G. Uestuenisik, Y. Sarikaya, J. Therm. Anal. Calorim. 89 (2007) 169–174.
[25] L. Pérez-Maqueda, J. Poyato, J. Pérez-Rodríguez, J. Therm. Anal. Calorim. 78 (2004) 375–383.
[26] L.A. Pérez-Maqueda, J.M. Blanes, J. Pascual, J.L. Pérez-Rodríguez, J. Eur. Ceram. Soc. 24 (2004) 2793–2801.
[27] L.A. Pérez-Maqueda, O.M. Montes, E.M. González-Macias, F. Franco, J. Poyato, J.L. Pérez-Rodríguez, Appl. Clay Sci. 24 (2004) 201–207.
[28] J.L. Pérez-Rodríguez, J. Pascual, F. Franco, M.C. Jiménez de Haro, A. Duran, V. Ramírez del Valle, L.A. Pérez-Maqueda, J. Eur. Ceram. Soc. 26 (2006) 747–753.
[29] M. Shirvani, F. Nourbakhsh, Appl. Clay Sci. 48 (2010) 393–397.
[30] J.M. Cases, Y. Grillet, M. François, L. Michot, F. Villiéras, J. Yvon, Clays Clay Miner. 39 (1991) 191–201.
[31] E. Garcia-Romero, M. Suarez, Clays Clay Miner. 58 (2010) 1–20.
[32] M. Suarez, E. Garcia-Romero, Appl. Clay Sci. 31 (2006) 154–163.
[33] R.L. Frost, J. Kristof, E. Horvath, J. Therm. Anal. Calorim. 98 (2009) 423–428.
[34] H. Hayashi, R. Otsuka, N. Imai, Am. Miner. 54 (1969) 1613–1624.
[35] M. Sanchez del Rio, E. Boccaleri, M. Milanesio, G. Croce, W. van Beek, C. Tsiantos, G.D. Chyssikos, V. Gionis, G.H. Kacandes, M. Suarez, E. Garcia-Romero, J. Mater. Sci. 44 (2009) 5524–5536.
[36] W. Kuang, G.A. Facey, C. Detellier, Clays Clay Miner. 52 (2004) 635–642.
[37] S. Mojumdar, J. Therm. Anal. Calorim. 64 (2001) 1133–1139.
[38] E.T. Stepkowska, J.L. Pérez-Rodríguez, M.J. Sayagués, J.M. Martínez-Blanes, J. Therm. Anal. Calorim. 73 (2003) 247–269.